Molecular Cell, Volume *31*

Supplemental Data

Caenorhabditis elegans drp-1 and *fis-2* Regulate Distinct Cell Death Execution Pathways Downstream of *ced-3* and Independent of *ced-9*

David G. Breckenridge, Byung-Ho Kang, David Kokel, Shohei Mitani, L. Andrew Staehelin, and Ding Xue

Supplemental Experimental Procedures

Strains and culture conditions

Strains of *C. elegans* were maintained at 20°C using standard protocols (Brenner, 1974). *N2* was the wild type stain. Alleles of *ced-3*, *ced-4* and *ced-9* used in this study have been described previously (1997). *eat-3(ad426)* and *fis-2(gk363)* mutants were obtained from *Caenorhabditis* Genetics Center (CGC) (Avery, 1993). *eat-3(tm1107)*, *fzo-1(tm1133)*, *drp-1(tm1108)*, *fis-1(tm1867)*, *fis-1(tm2227)*, and *fis-2(tm1832)* animals were obtained from Japan National Bioresource Project (NBRP). All strains were backcrossed with *N2* animals 5-10 times prior to analysis. *cps-6* and *wah-1* RNAi treatment was carried out using a bacterial feeding protocol as previously described (Kamath et al., 2001; Wang et al., 2002). Animals were subjected to two generations of RNAi treatment and F2 progeny were scored for the cell death defects.

Molecular Biology

P_{hsp}*egl-l*, P_{hsp} *drp-1*, and P_{hsp}*fis-2* expression vectors were constructed by subcloning the respective full-length cDNAs into the pPD49.78 and pPD49.83 vectors, which harbor the *C. elegans hsp-16.2* and *hsp-16.41* promoters, respectively. To construct P_{hsp}*gfp::fis-2*, a

coding region for the Green Fluorescent Protein (GFP) was amplified from the pPD95.79 vector and subcloned into the pPD49.78 and pPD49.83 vectors, creating pPD49.78-GFP and pPD49.83-GFP constructs. Full-length *fis-2* cDNA was then subcloned into the pPD49.78-GFP and pPD49.83-GFP vectors as a carboxyl terminal fusion to GFP. *drp-1* cDNA was amplified by polymerase chain reaction (PCR) from a *C. elegans* cDNA library and cloned into the pDONR221 donor and the pDEST14 destination gateway vectors according to the manufacturers protocols (Invitrogen). The 3994 bp *drp-1* genomic rescuing construct (containing 963 bp of sequence upstream of the initiation ATG codon and 479 bp downstream of the termination codon) was amplified by PCR from the fosmid clone wrm0628dc05 and cloned into pDONR221, creating the pENTR-*drp-1*(+) construct. Constructs containing the D118A mutation were created using standard site-directed mutagenesis techniques. PCR amplification and the gateway cloning method were used to create a gateway entry vector containing *drp-1*(119-712), pENTR-*drp-1*(119-712), which also includes introns and 479 bp of sequence after the termination codon. *drp-1*(119-712) was then placed under the control of the 963 bp *drp-1* promoter by performing an LR reaction between pENTR-*drp-1*(119-712) and a P_{drp-1}DEST vector.

Transgenic Animals

Plasmids (2-25 µg/ml) were injected into *unc-76(e911),* N2, *drp-1(tm1108) ced-3(n2438), or ced-4(n2273); drp-1(tm1108)* animals with p76-16B (25 µg/ml), a construct that rescues the *unc-76(e991)* mutant, or with pRF4 (25 µg/ml), a dominant *rol-6* construct, or with P_{myo-3}MitoGFP (Labrousse et al., 1999) as co-injection markers. For the

rescuing experiments with *drp-1(tm1108) ced-3(n2438)* animals, *drp-1*(+) or *drp-1*(D118A) constructs were injected at 10 µg/ml, while *drp-1*(D118A) and *drp-1*(119-712) constructs were co-injected at 10 µg/ml and 2 µg/ml, respectively. Stable transgenic lines of non-Unc animals, Roller animals, or GFP transgenic animals were then selected. An integrated line containing the P_{hsp}*egl-1* constructs (*smIs82*) or the P_{egl-1}acCED-3 construct (*smIs111)* was obtained by irradiating the animals with the corresponding extrachromosomal arrays with gamma rays and screening for progeny with 100% inheritance of the transgene. Integrants were backcrossed with N2 animals five times prior to crossing into the various mitochondrial fission and fusion mutants. For the heat-shock experiments, heat-shock treatment of animals was carried out as previously described (Jagasia et al., 2005) and the number of cell corpses at the 1.5-fold stage embryos was counted 2-3 hours post the heat-shock treatment.

Live imaging of *C. elegans* mitochondria and electron microscopy

Labeling of mitochondria with tetramethylrhodamine ester (TMRE; Molecular Probes) was carried out as previously described (Jagasia et al., 2005). Embryos were dissected from gravid adults on a 2% agar pad soaked in M9 buffer and visualized using an Axioplan 2 Nomarski Microscope (Carl Zeiss MicroImaging Inc., Thorton, NY, USA) equipped with a SensiCam CCD camera and slidebook 4.0 software (Intelligent Imaging Innovations, Denver, CO, USA). Imaging MitoGFP in body wall muscle cells was done as described previously (Labrousse et al., 1999). For visualization of mitochondria by electron microscopy, adult worms were mixed with *E. coli* and loaded into type B high-pressure freezing planchettes (Baltec, Tucson, AZ). After cryofixed by Baltec HPM010

high-pressure freezer, the samples were freeze-substituted in anhydrous acetone containing 2% osmium tetroxide at –80^{o}C for 4 days and slowly warmed to room temperature over 48 hours. Infiltration with EPON/Araldite resin (Ted Pella, Reddings, CA), mounting, sectioning, and post-staining were performed essentially as described (Muller-Reichert et al., 2003). Worms and embryos were observed with a Philips (Hillsboro, OR) CM10 electron microscope operated at 80 kV. To prepare 4-fold stage embryos for EM sectioning, adult hermaphrodite animals were starved 5-6 hours prior to fixation so that embryos could mature and accumulate in the uterus of animals. Quantification of EM sections was preformed with Image J software. Mitochondrial length was estimated by measuring the longest longitudinal axis of randomly selected mitochondria. For each strain, mitochondria were selected from over 10 different embryos inside at least two thin-sectioned gravid adult animals. The mean length of mitochondria in *drp-1(tm1108)* animals is likely to be highly underestimated because as the length of an individual mitochondrion increases, the chance of capturing the entire organelle in a single thin sectioned plane decreases. In cases where serial sectioning was employed, the section in which a given mitochondria appeared largest was chosen for measurement. To quantify mitochondria in cell corpses, a single section through each cell corpse was chosen at random and the number of individual mitochondria in that section was counted. This method was adopted instead of quantifying the total number of mitochondria observed in serial sections through a cell corpse, because it rules out bias that may be attained if a series of sections does not go completely through a cell corpse and allows a greater sampling number. To obtain the mitochondrial area index, serial sections through a cell corpse were analyzed and the sections where each mitochondrion

appeared largest were chosen for area measurement. The areas of each mitochondrion measured in a cell corpse were added and then divided by the total area of the corpse (measured from the section where the corpse area appeared largest).

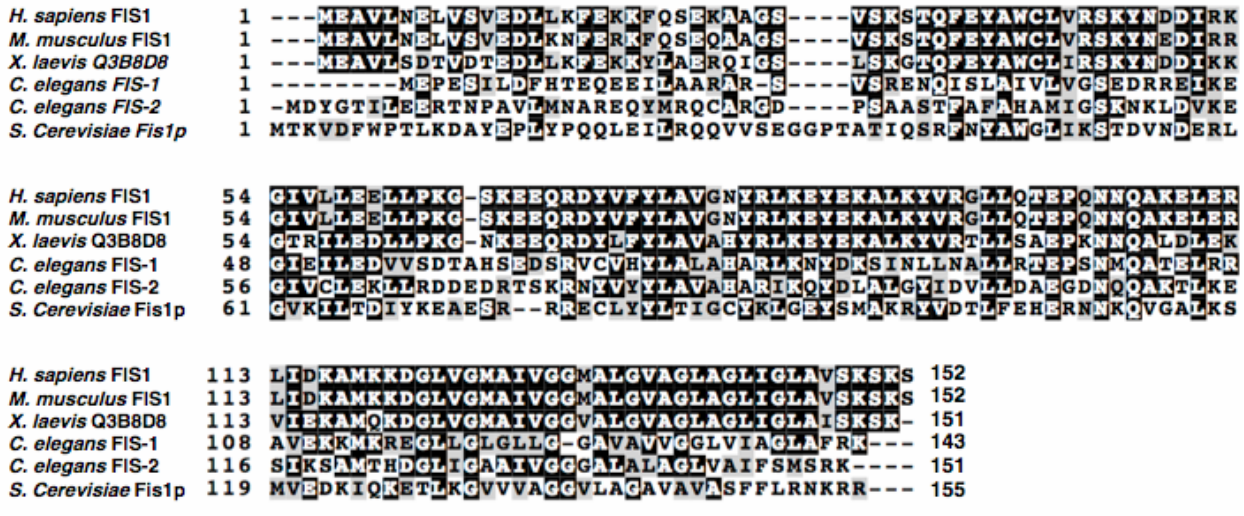

Figure S1. Alignment of Fis genes from human, mouse, *X. laevis*, *C. elegans*, and *S. cerevisiae*. Sequences were aligned and shaded using the ClustalW and BoxShade programs, respectively. Identical residues are shaded in black and conserved residues are shaded in grey.

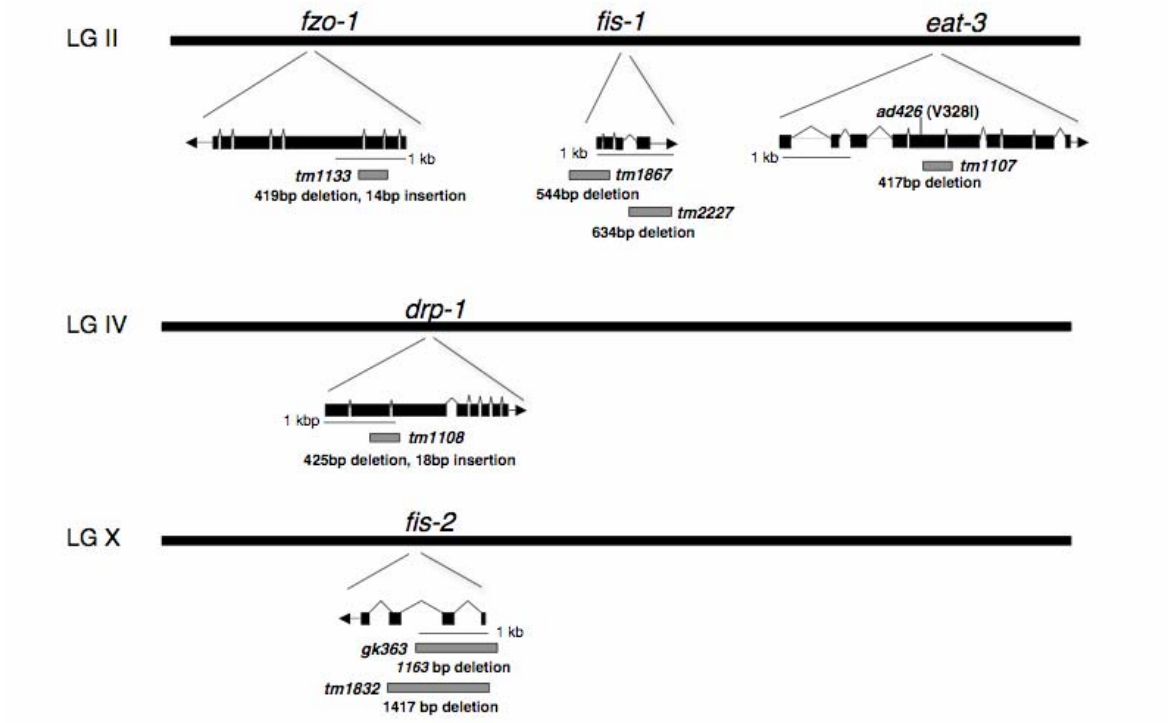

Figure S2. Schematic representations of deletions or mutations in the mitochondrial fission and fusion genes. LG, linkage group. Black boxes represent exons and waved lines indicate introns. Arrows pointed away from the boxes indicate the direction of transcription. Grey boxes represent the regions removed in each deletion allele. The actual size of each deletion (and in some cases with insertion) is indicated below the grey boxes.

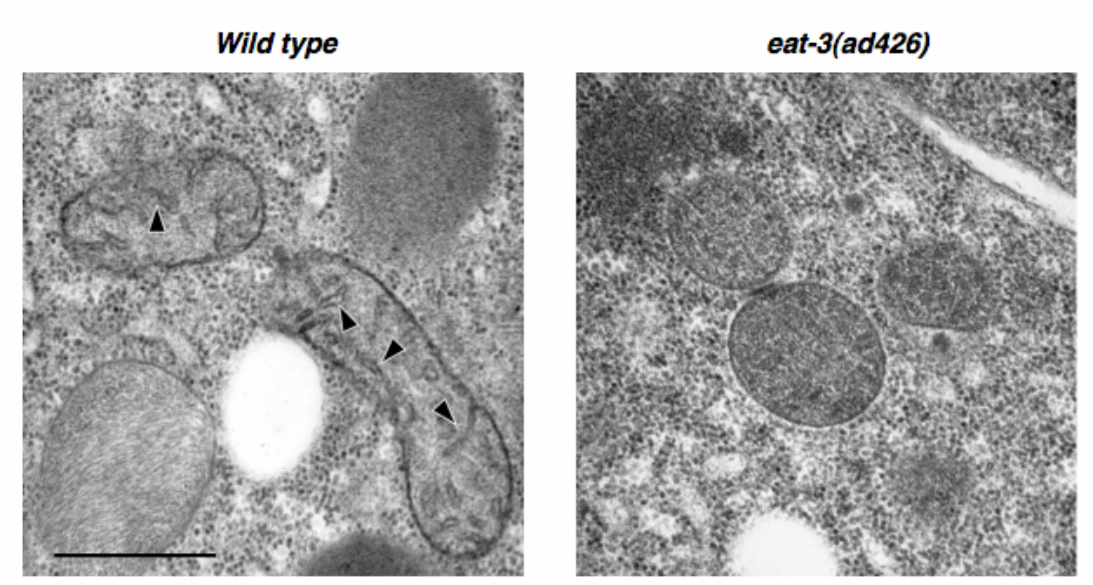

Figure S3. Disrupted cristae structure in the *eat-3(ad426)* mutant. Electron micrographs of the wild type (left) and the *eat-3(ad426)* (right) embryos. Arrowheads indicate normal cristae structure in mitochondria of the wild type embryo, which are absent or severely disrupted in mitochondria of the *eat-3(ad426)* embryo. Scale bar represents 0.5 μM.

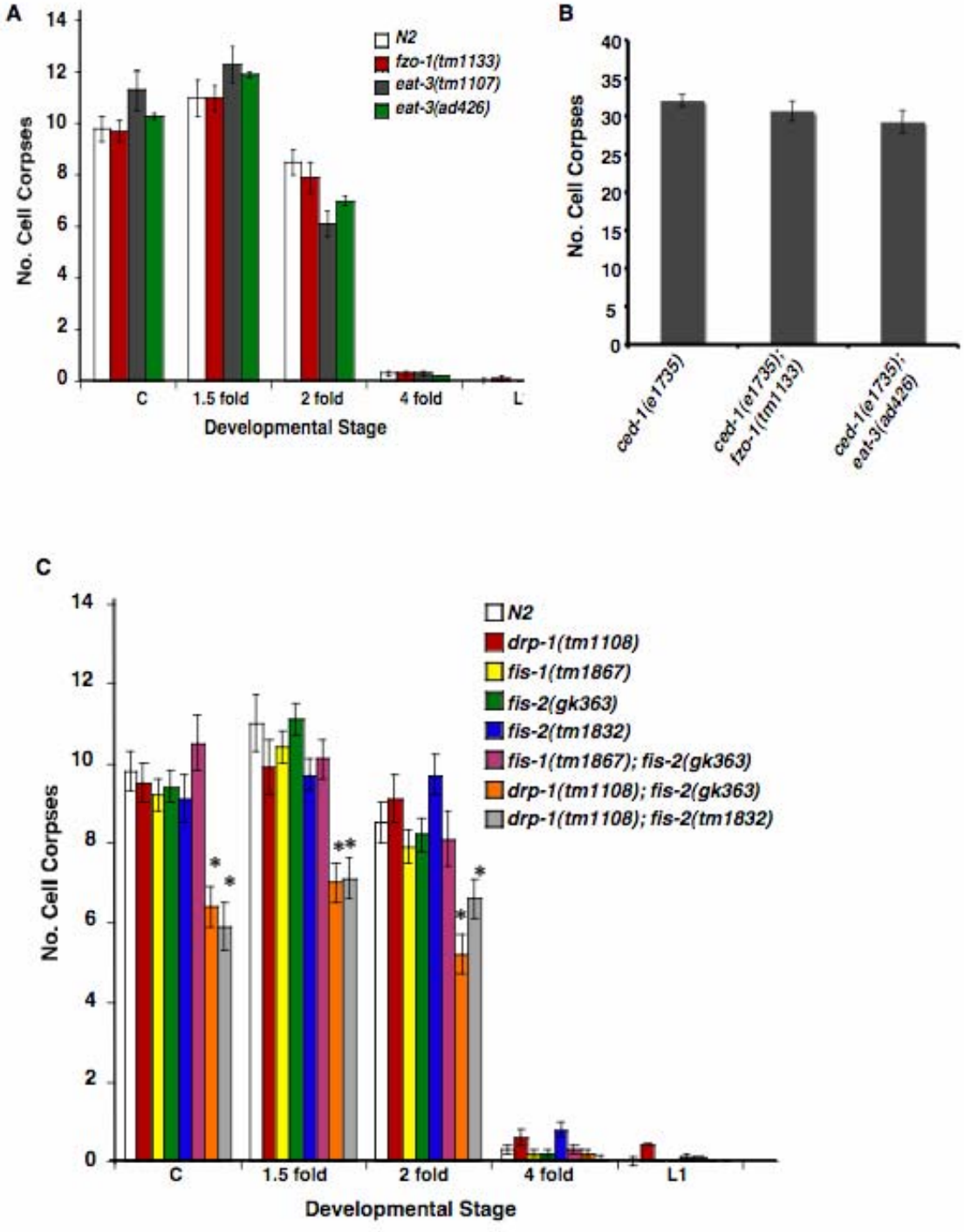
A
No. Cell Corpses
Developmental Stage
C
1.5 fold
2 fold
4 fold
L
N2
fzo-1(tm1133)
eat-3(tm1107)
eat-3(ad426)
B
No. Cell Corpses
ced-1(e1735)
ced-1(e1735); fzo-1(tm1133)
ced-1(e1735); eat-3(ad426)
C
No. Cell Corpses
Developmental Stage
C
1.5 fold
2 fold
4 fold
L1
N2
drp-1(tm1108)
fis-1(tm1867)
fis-2(gk363)
fis-2(tm1832)
fis-1(tm1867); fis-2(gk363)
drp-1(tm1108); fis-2(gk363)
drp-1(tm1108); fis-2(tm1832)

Figure S4. The kinetics of embryonic cell corpse appearance is not affected in the individual mitochondrial fission or fusion mutants. (A) Time-course analysis of cell corpse appearance during embryonic development in mitochondrial fusion mutants. Cell corpses were counted at the comma (C), 1.5-fold, 2-fold, and 4-fold embryonic stages, and the L1 larval stage. The Y-axis indicates the mean number of cell corpses scored in the head region of embryos or larvae. 15 animals were scored at each stage. (B) Analysis of the cell corpse numbers of mitochondrial fusion mutants in a sensitized *ced-1(e1735)* mutant background, which is defective in engulfment of cell corpses. Animals were scored as in (A) at the 4-fold stage embryos. (C) Time-course analysis of embryonic cell corpse appearance in *drp-1, fis-1* and *fis-2* mutants and corresponding double mutants. Cell corpses were counted as in (A). In all panels, error bars indicate the standard error of the mean. * Unpaired two tailed *t*-test, N2 vs. *drp-1(tm1108); fis-2(gk363)* at the comma, 1.5-fold and 2-fold stages: $P=2.8x10^{-5}$, $5.2x10^{-5}$, and $2.9x10^{-4}$, respectively; N2 vs. *drp-1(tm1108);fis-2(tm1832)* at the comma, 1.5 fold and 2 fold stages: $P=2.3x10^{-5}$, $9.8x10^{-5}$, and 0.043, respectively.

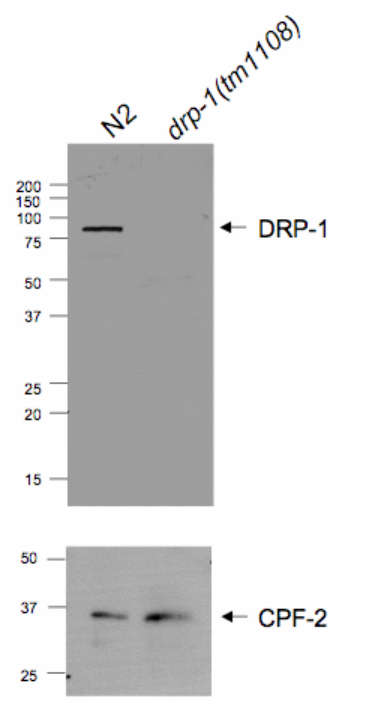

Figure S5. The *drp-1(tm1108)* deletion mutation results in a complete loss of the DRP-1 protein. Total worm lysates from *N2* and *drp-1(tm1108)* animals were resolved on a 10% SDS polyacrylamide gel, transferred to a nitrocellulose membrane, and then probed with anti-DRP-1 antibody (see Experimental Procedures). The CPF-2 protein was used as a loading control (Evans et al., 2001).

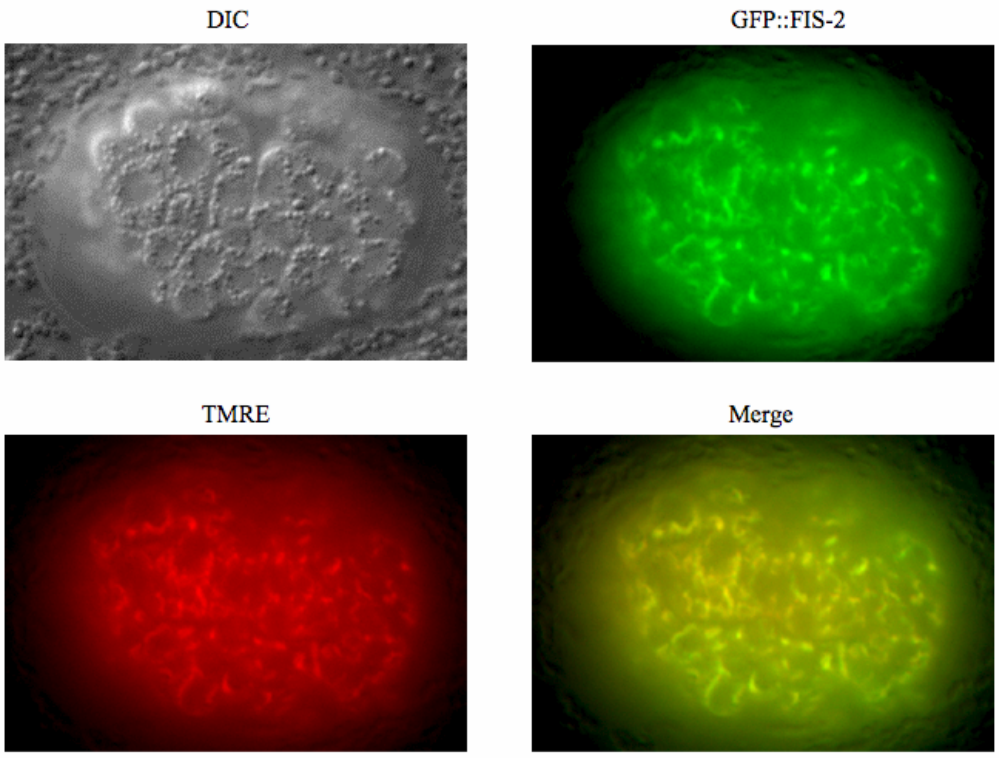

Figure S6. GFP::FIS-2 localizes to mitochondria in *C. elegans*. An embryo transgenic for the P_{hsp}*gfp::fis-2* constructs was stained with the mitochondria-specific dye TMRE, subjected to the heat-shock treatment to induce the expression of the GFP::FIS-2 fusion, and then visualized by fluorescent microscopy with Rhodamine and FITC filters. The merged image of GFP::FIS-2 and TMRE staining reveals extensive co-localization of GFP::FIS-2 with TMRE.

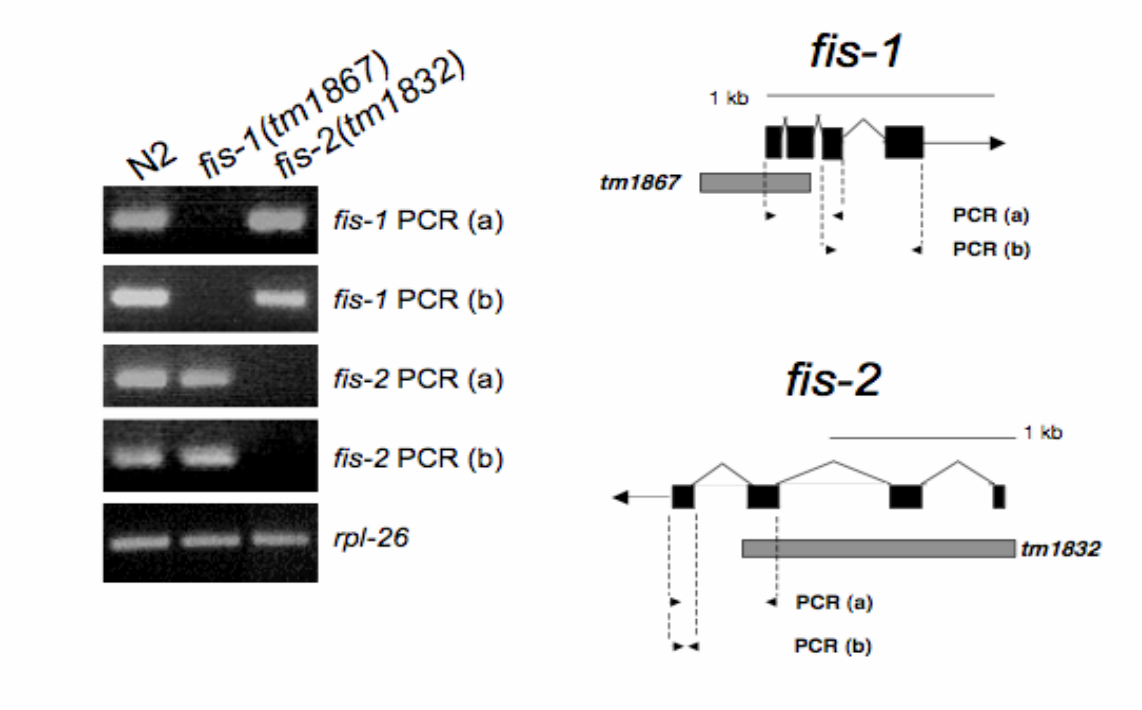

Figure S7. *fis-1(tm1867)* and *fis-2(tm1832)* deletion mutations result in complete loss of *fis-1* and *fis-2* expression, respectively. Reverse transcription was preformed on purified poly(A)$_n$ mRNA isolated from *N2, fis-1(tm1867),* and *fis-2(tm1832)* animals, followed by PCR amplification with primers specific to the coding regions of either *fis-1*, *fis-2*, or a control gene *rpl-26* (encoding a large ribosomal subunit L26 protein). The amplified PCR products in relation to the *fis-1* and *fis-2* genes are shown on the left. In each case, PCR (a) was conducted with one primer that is specific for a region within the respective gene deletion and one primer that lies outside of the deletion, whereas PCR (b) was conducted with primers lying outside of the gene deletions.

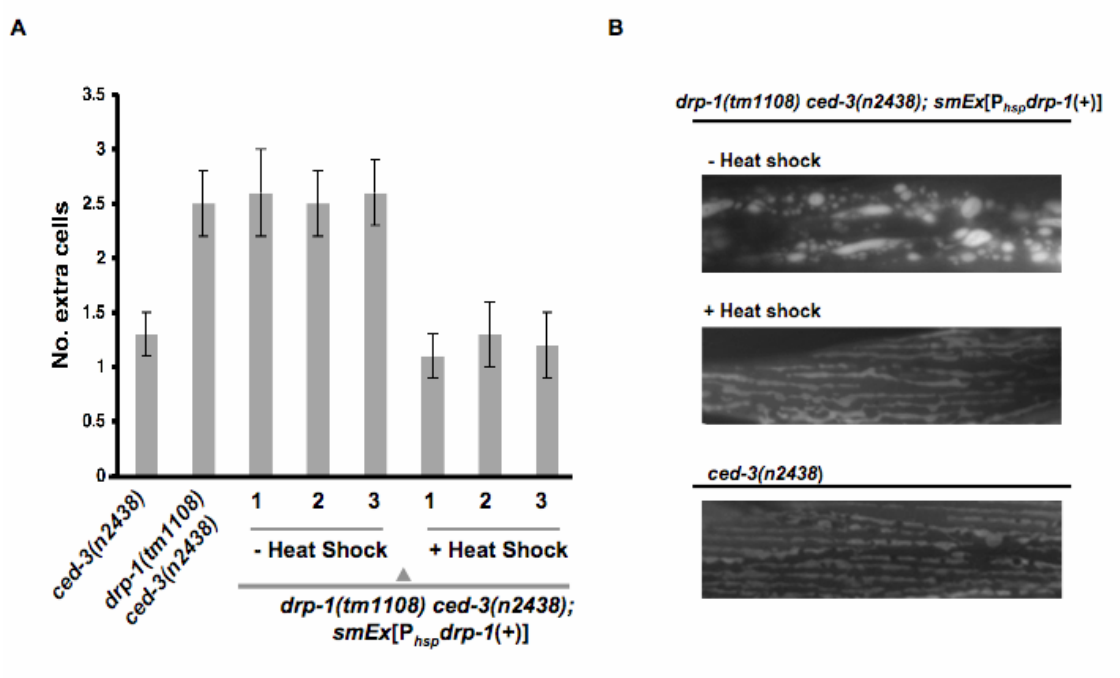

Figure S8. Overexpression of *drp-1* rescues the enhanced cell death defect in *drp-1(tm1108) ced-3(n2438)* animals. A) Three independent lines of *drp-1(tm1108) ced-3(n2438)* animals carrying a P_{hsp}*drp-1*(+) transgene were subjected to the heat-shock treatment (+ Heat Shock) at the embryonic stage as described in the Experimental Procedures or were not treated with heat-shock (- Heat Shock). The resulting larvae were analyzed for the number of extra cells in the anterior pharynx. Error bars indicate s.e.m. B). Overexpression of *drp-1* rescues the mitochondrial fission defect in *drp-1(tm1108) ced-3(n2438)* animals. Experiments were carried out as in (A), except that the embryos were allowed to develop into young adults and the muscle cell mitochondria labeled by P_{myo-3}*MitoGFP* were visualized by fluorescence microscopy.

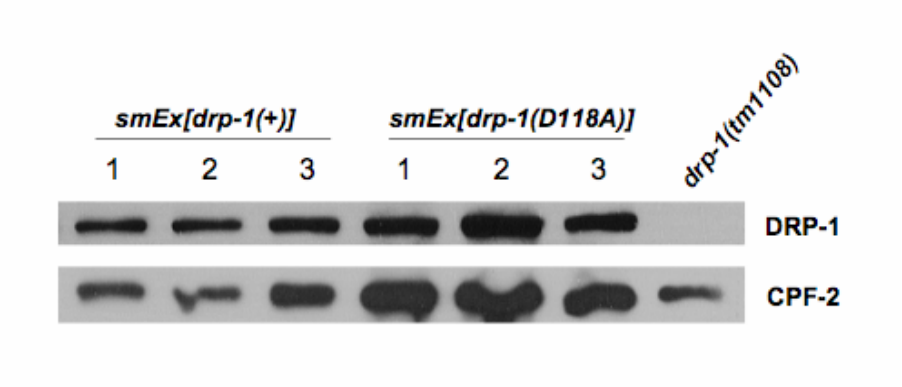

Figure S9. *drp-1*(+) and *drp-1*(D118A) transgenes express similar levels of the DRP-1 protein. Total worm lysates from three independent lines of *drp-1(tm1108) ced-3(n2438)* animals carrying either *smEx*[*drp-1*(+)] or *smEx*[*drp-1*(D118A)] transgenes were resolved on a 10% SDS polyacrylamide gel, transferred to a nitrocellulose membrane, and then probed with anti-DRP-1 antibody (see Experimental Procedures). The CPF-2 protein was used as a loading control (Evans et al., 2001).

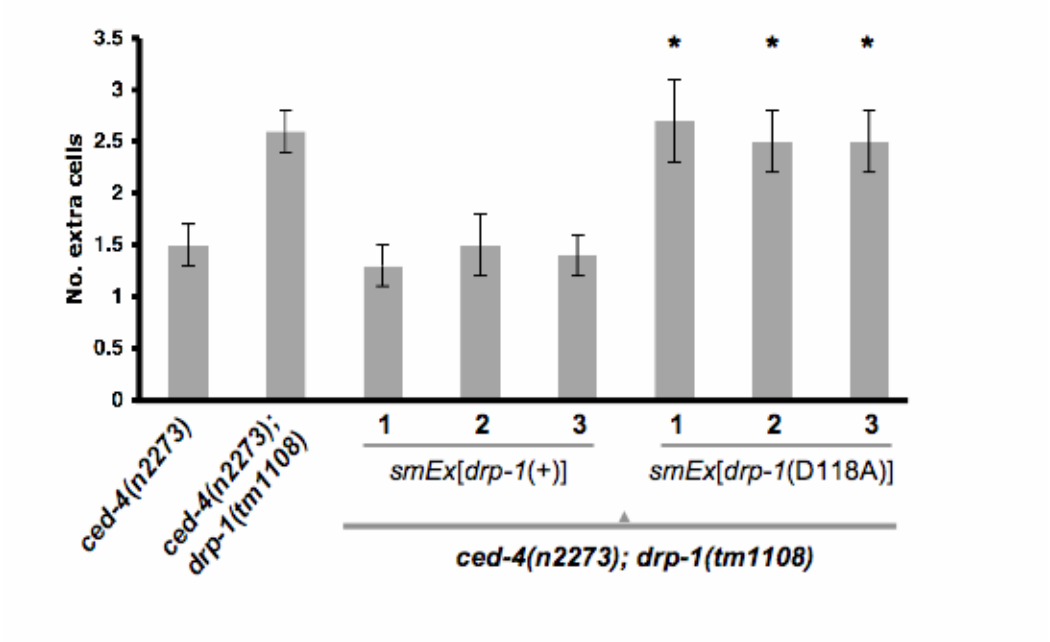

Figure S10. The enhanced cell death defect in *ced-4(n2273); drp-1(tm1108)* animals is rescued by *drp-1*(+) transgenes but not by *drp-1*(D118A) transgenes. *ced-4(n2273)*; *drp-1(tm1108)* animals carrying transgenes containing a 3994 bp *drp-1* genomic fragment [*drp-1*(+)] or the *drp*-1 genomic fragment harboring the DRP-1^{D118A} mutation [*drp-1*(D118A)] were analyzed for the number of extra cells in the anterior pharynx. Three independent transgenic lines were examined for each construct. Error bars indicate s.e.m. Unpaired two tailed *t*-test, compared with *ced-4(n2273)* animals: * $P < 0.005$.

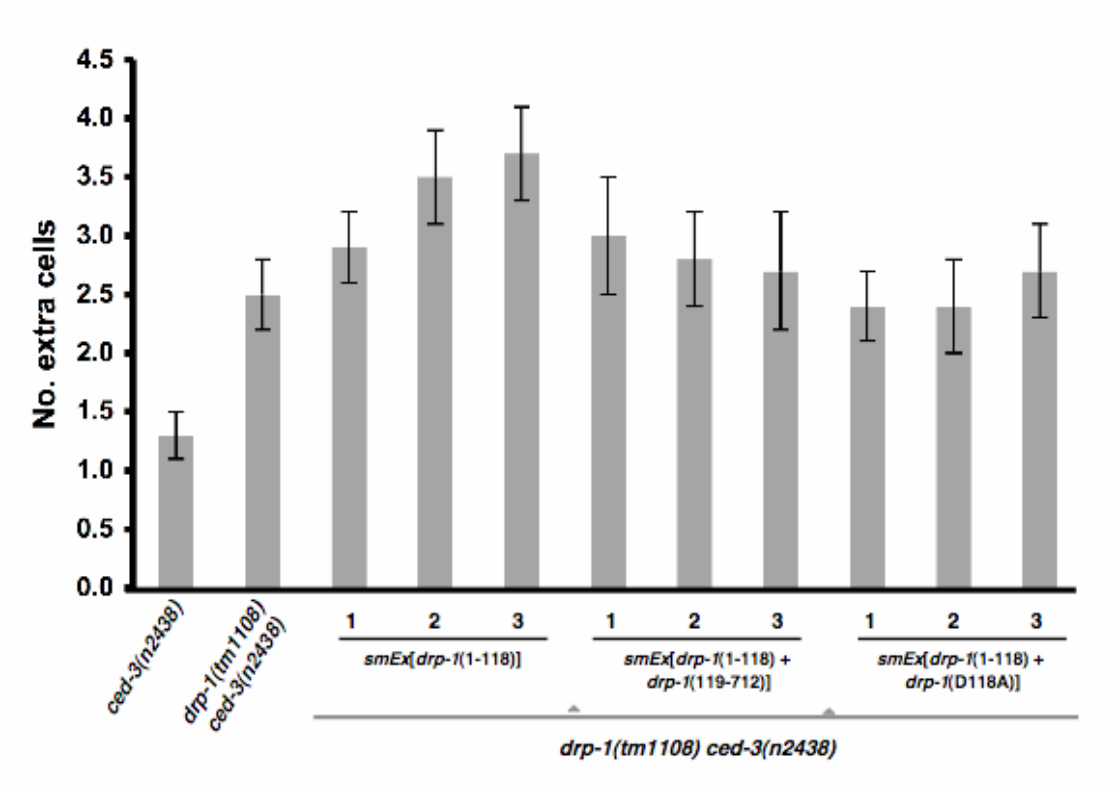

Figure S11. Expression of *drp-1*(1-118) or *drp-1*(119-712) alone or together does not rescue the enhanced cell death defect in *drp-1(tm1108) ced-3(n2438)* animals. *drp-1(tm1108) ced-3(n2438)* animals carrying the indicated transgene were analyzed for the number of extra cells in the anterior pharynx. Three independent transgenic lines were examined for each transgene. Error bars indicate s.e.m.

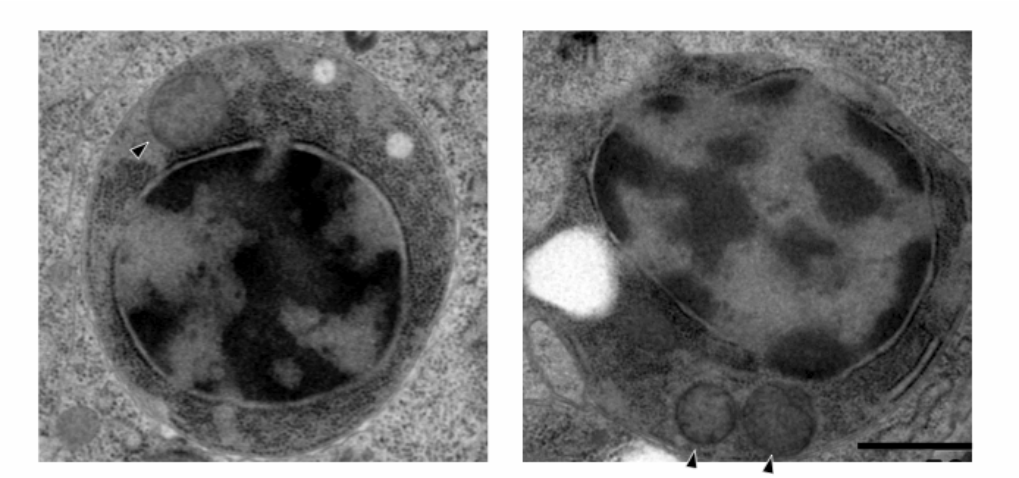

Figure S12. Mitochondria are fragmented in *ced-1(e1735); drp-1(tm1108)* corpses in the absence of DRP-1. The arrowhead marks a small and spherical mitochondrion similar to the ones seen in *ced-1(e1735)* cell corpses. Scale bar represents 0.5 μm.

Table S1. Overexpression of *drp-1*(K40A) inhibits apoptosis in *drp-1(tm1108)* animals to the same extent as in wild-type animals.

Genotype	Number of extra cells			
	Mean	s.e.m.	Range	n
N2	0.1	0.1	0-1	40
drp-1(tm1108)	0.1	0.1	0-1	30
+/+; *smEx*[P_{hsp}*drp-1*(K40A)] #1 - HS	0.1	0.1	0-1	20
+/+; *smEx*[P_{hsp}*drp-1*(K40A)] #2 - HS	0.1	0.1	0-1	20
+/+; *smEx*[P_{hsp}*drp-1*(K40A)] #3 - HS	0	0	0	20
+/+; *smEx*[P_{hsp}*drp-1*(K40A)] #4 - HS	0.1	0.1	0-1	20
+/+; *smEx*[P_{hsp}*drp-1*(K40A)] #1 + HS	1.2	0.2	0-3	20
+/+; *smEx*[P_{hsp}*drp-1*(K40A)] #2 + HS	1.0	0.1	0-3	20
+/+; *smEx*[P_{hsp}*drp-1*(K40A)] #3 + HS	0.8	0.2	0-3	20
+/+; *smEx*[P_{hsp}*drp-1*(K40A)] #4 + HS	1.0	0.2	0-3	20
drp-1(tm1108); smEx[P_{hsp}*drp-1*(K40A)] #1 - HS	0.1	0.1	0-1	20
drp-1(tm1108); smEx[P_{hsp}*drp-1*(K40A)] #2 - HS	0.1	0.1	0-1	20
drp-1(tm1108); smEx[P_{hsp}*drp-1*(K40A)] #3 - HS	0.2	0.1	0-1	20
drp-1(tm1108); smEx[P_{hsp}*drp-1*(K40A)] #4 - HS	0.1	0.1	0-1	20
drp-1(tm1108); smEx[P_{hsp}*drp-1*(K40A)] #1 + HS	0.8	0.2	0-2	20
drp-1(tm1108); smEx[P_{hsp}*drp-1*(K40A)] #2 + HS	1.1	0.2	0-3	20
drp-1(tm1108); smEx[P_{hsp}*drp-1*(K40A)] #3 + HS	1.0	0.2	0-3	20
drp-1(tm1108); smEx[P_{hsp}*drp-1*(K40A)] #4 + HS	0.9	0.2	0-2	20

Animals were injected with a construct that expresses *drp-1(K40A)* under the control of the heat-inducible promoter (P_{hsp}). Heat-shock treatment (+ HS) was carried out as described by Jagasia et al. (2005) and the number of extra cells in the anterior pharynx of the transgenic animals was scored as described in Experimental Procedures. For each experiment [with or without heat-shock treatment (- HS) or in wild-type (+/+) or *drp-1(tm1108)* background], four independent transgenic lines were scored (indicated by #). s.e.m., standard error of the mean. n indicates the number of transgenic animals scored.

Table S2. Overexpression of *fis-2* induces ectopic apoptosis independent of *drp-1*

Genotype	Number of cell corpses			
	Mean	s.e.m.	Range	n
N2	10.4	0.6	7-13	15
N2 (heat-shock control)	10.7	0.7	7-15	15
+/+; *smEx*[P_{hsp}*drp-1*] #1	8.4	0.5	5-13	15
+/+; *smEx*[P_{hsp}*drp-1*] #2	9.0	0.5	6-16	15
+/+; *smEx*[P_{hsp}*drp-1*] #3	9.6	0.8	6-18	15
+/+; *smEx*[P_{hsp}*fis-2*] #1	19.1	0.7	14-24	15
+/+; *smEx*[P_{hsp}*fis-2*] #2	14.1	1.2	8-23	15
+/+; *smEx*[P_{hsp}*fis-2*] #3	18.2	1.1	10-28	15
drp-1(tm1108); *smEx*[P_{hsp}*fis-2*] #1	18.3	0.9	11-25	15
drp-1(tm1108); *smEx*[P_{hsp}*fis-2*] #2	15.2	0.5	13-19	15
drp-1(tm1108); *smEx*[P_{hsp}*fis-2*] #3	17.2	0.8	12-23	15
+/+; *smEx*[P_{hsp}*fis-2*(1-124] #1	8.7	0.4	6-11	15
+/+; *smEx*[P_{hsp}*fis-2*(1-124] #2	8.6	0.4	6-11	15
+/+; *smEx*[P_{hsp}*fis-2*(1-124] #3	8.8	0.5	6-12	15

Animals were injected with the indicated construct that expresses *drp-1*, *fis-2*, or *fis-2(1-124)* under the control of the heat-inducible promoters. Protein expression was induced by heat-shock treatment at 33ºC for 40 minutes as described by Jagasia et al. (2005) and the number of cell corpses in the head region of 1.5-fold stage embryos was scored. For each experiment, three independent transgenic lines were scored (indicated by #). s.e.m., standard error of the mean. n indicates the number of transgenic embryos scored.

REFERENCES

C. elegans II (1997). Cold Spring Harbor Laboratory, Cold Spring Harbor.
Avery, L. (1993). The genetics of feeding in *Caenorhabditis elegans*. Genetics *133*, 897-917.
Brenner, S. (1974). The genetics of Caenorhabditis elegans. Genetics *77*, 71-94.
Evans, D., Perez, I., MacMorris, M., Leake, D., Wilusz, C. J., and Blumenthal, T. (2001). A complex containing CstF-64 and the SL2 snRNP connects mRNA 3' end formation and trans-splicing in *C. elegans* operons. Genes Dev. *15*, 2562-2571.
Jagasia, R., Grote, P., Westermann, B., and Conradt, B. (2005). DRP-1-mediated mitochondrial fragmentation during EGL-1-induced cell death in *C. elegans*. Nature *433*, 754-760.
Kamath, R. S., Martinez-Campos, M., Zipperlen, P., Fraser, A. G., and Ahringer, J. (2001). Effectiveness of specific RNA-mediated interference through ingested double-stranded RNA in *Caenorhabditis elegans.* Genome Biol. *2*, RESEARCH0002.
Labrousse, A. M., Zappaterra, M. D., Rube, D. A., and van der Bliek, A. M. (1999). *C. elegans* dynamin-related protein DRP-1 controls severing of the mitochondrial outer membrane. Mol. Cell *4*, 815-826.
Muller-Reichert, T., Hohenberg, H., O'Toole, E. T., and McDonald, K. (2003). Cryoimmobilization and three-dimensional visualization of *C. elegans* ultrastructure. J. Microsc. *212*, 71-80.
Wang, X., Yang, C., Chai, J., Shi, Y., and Xue, D. (2002). Mechanisms of AIF-mediated apoptotic DNA degradation in *Caenorhabditis elegans*. Science *298*, 1587-1592.